

Machining Time Dependent Chip Behavior and Hole Accuracy in Drilling Aluminum 5083 Alloy

Humayra Jannat Tuba

Industrial Engineering and Management Department
Khulna University of Engineering and Technology
Khulna, Bangladesh
jannattuba16@gmail.com

Nazma Sultana

Associate Professor
Department of Industrial Engineering and Management
Khulna University of Engineering and Technology
Khulna, Bangladesh
n.sultana@iem.kuet.ac.bd

Nizam Uddin Ahmed

Industrial Engineering and Management Department
Khulna University of Engineering and Technology
Khulna, Bangladesh
nu563999@gmail.com

Abstract

In manufacturing, the progressive deterioration of hole quality during drilling particularly in aluminum alloys such as Al-5083 is a critical concern due to its direct impact on assembly accuracy and tolerance control. This study investigates how machining time influences drilled hole geometry, while establishing the role of chip behavior as an in-process indicator of drilling stability. A total of 52 consecutive holes were drilled using a High-Speed Steel (HSS) tool, and three geometric quality measures such as circularity, cylindricity, and conicity were evaluated for each hole. In addition, the interrelationship among these geometric errors was examined. Throughout the drilling sequence, chip morphology exhibited a clear transition from ideal, continuous ribbons in the initial stage to unstable “Transition chips” as machining progressed. Although the geometric errors did not show strong trends in isolation, the occurrence of transition chips consistently coincided with the largest deviations in hole geometry. Notably, these unstable chips were responsible for approximately 75% of holes that failed to meet industrial tolerance limits. The findings highlight that chip morphology serves as a practical real-time indicator of drilling stability and final hole quality, offering a valuable complement to traditional post-process geometric inspection.

Keywords

Drilling, Machining time, Hole Accuracy, Chip Morphology, Tool wear.

1. Introduction

Aluminum 5083 (Al–Mg) is extensively employed in marine structures, pressure vessels, transportation systems, and other load-bearing applications due to its high strength, notable corrosion resistance, and favorable formability (Gloria A, 2019). As a non-heat-treatable alloy, its mechanical properties arise primarily from solid-solution strengthening

and work hardening (J. Hirsch, 2013). With the increasing use of lightweight structural materials, the machining performance of Al5083 has become an important consideration, particularly for drilling operations where dimensional accuracy and assembly precision are critical. Drilling aluminum alloys is often complicated by their low melting temperature, high thermal conductivity, and pronounced tendency for material adhesion (Dursun T, 2014). These factors promote the formation of built-up edge (BUE) and welded chips on the cutting tool, which alter the effective cutting geometry and may lead to increased cutting forces, surface deterioration, and deviations in geometric tolerances such as circularity, cylindricity, and conicity (Oliaei, S. 2016) (Davoudinejad, 2017). In the case of Al5083, long continuous chips and adhesive wear are frequently reported, making the alloy susceptible to tolerance variation during extended machining cycles (Aamir,2020). Machining time further affects hole integrity by influencing thermal conditions, tool–workpiece interaction, and the progression of tool wear. Prolonged cutting can induce rapid thermal fluctuations due to the alloy’s high thermal conductivity, which may introduce residual stress and compromise dimensional stability (Ramme J, 2022). Chip morphology, including chip form and chip thickness ratio offers useful insight into the prevailing cutting mechanics and tool-wear state, and has been shown to correlate with the geometric accuracy of drilled holes (Batzer 1998). A clear understanding of these relationships is essential for the selection of appropriate drilling parameters and for improving the dimensional reliability of Al5083 components in precision applications.

2. Literature Review

Drilling of aluminum alloys has been widely studied to understand how tool type, cutting parameters, and drilling environments influence hole quality. (Ahmad, 2024) showed that feed rate affects circularity error in aluminum alloys, where higher feed rates increase deviations due to vibration and deflection, though notable variability also appeared at lower feeds. (Aamir, 2023) reported that drill-bit material plays a major role in circularity performance for Al2024-T3, and that higher feed rate and spindle speed reduce overall hole quality. (Kushnoore, 2016) analyzed circularity error in Al6061 and explained how drill diameter, spindle speed, and feed rate jointly influence geometric accuracy using RSM and ANOVA. Studies on Al7075 also show consistent trends: (Habib, 2021) found that feed rate dominates hole size, surface finish, and circularity, producing short segmented chips at high feed and low speed; (Abd Halim, 2020) observed that low cutting speed with cutting fluid improves tool wear and surface roughness compared to dry drilling; (Kao, 2019) demonstrated that inverted drilling reduces hole enlargement, improves roundness and surface roughness, and lowers tool wear, with spindle speed identified as the most influential parameter. Additional studies on drilling mechanics further confirm the critical role of process parameters: (Uddin, 2018) identified feed rate as the primary factor driving thrust force, torque, and dimensional accuracy; (Farid, 2011) established that higher cutting speeds significantly alter chip morphology due to built-up edge formation; (Müller, 2001) showed that chip segmentation in Al7075 depends on heat-treatment condition and cutting speed; and (Sharif, 2023) reported that both spindle speed and feed rate increase hole size and circularity, while high speed with low feed improves surface roughness. Despite these findings, very limited work has combined chip-formation behavior, circularity error, and machine-performance monitoring into a unified assessment of drilling quality for Al-5083 alloy under repeated dry-drilling conditions, which forms the motivation of the present study.

3. Materials and Method

3.1 Experimental Details

Aluminum 5083 was chosen as the workpiece material because of its favorable strength-to-weight ratio, corrosion-resistance and remarkably wide deployment in marine and aerospace applications (Figure 1, 2 and 3). Table 1 contains the results of the hardness measurement based on the Rockwell hardness test performed on the B scale with ball indenter and initial and total loads of 98.07 N and 980.7, respectively. The total elemental analysis in order to assess the elemental composition was performed using Energy Dispersive X-ray Spectroscopy (EDS) and results are shown in Table 2.

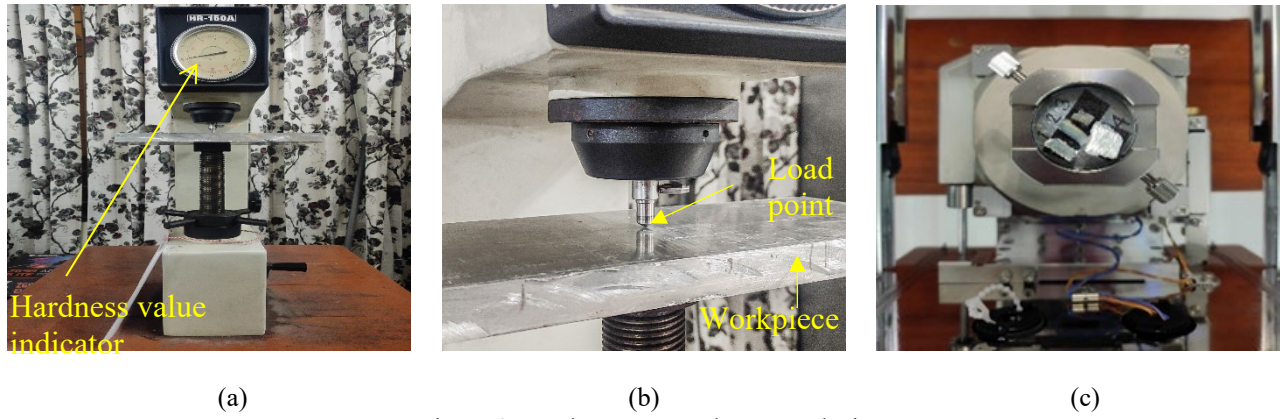


Figure 1: Hardness Test and EDS analysis

Table 1. Hardness Test Result (B scale)

| 1 st trial | 2 nd trial | 3 rd trial | 4 th trial | 5 th trial | 6 th trial |
|-----------------------|-----------------------|-----------------------|-----------------------|-----------------------|-----------------------|
| 90 | 104 | 80 | 121 | 95 | 119 |

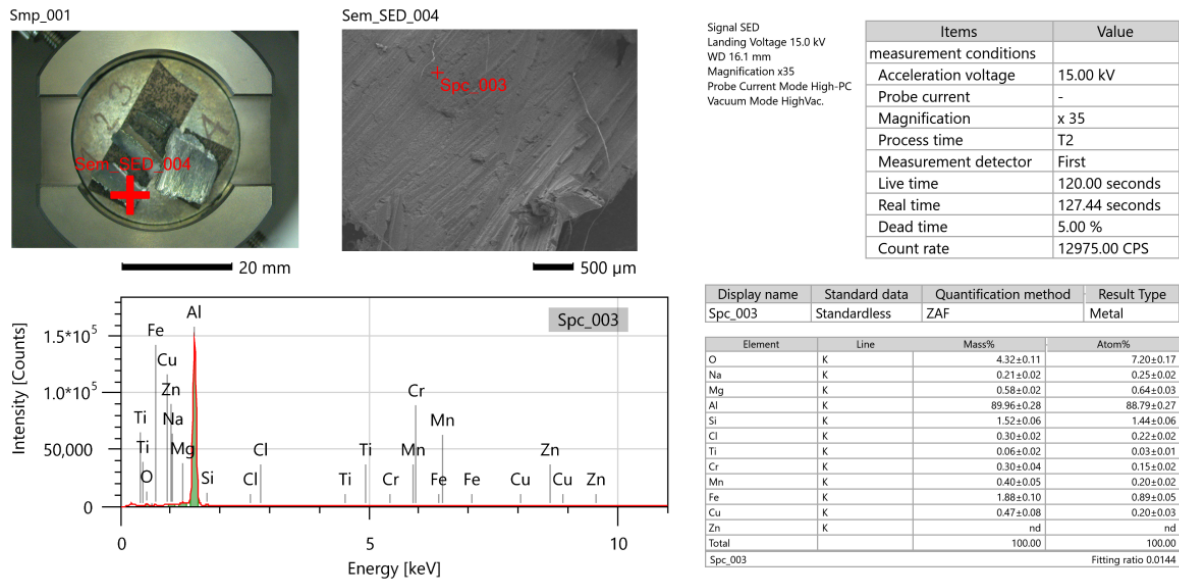


Figure 2: EDS result of the Al-5083 alloy

Table 2. Chemical composition of Al-5083 alloy

| Chemical elements | Al | O | Si | Fe | Mg | Cu | Mn | Cr | Cl | Na | Ti |
|-------------------|-------|------|------|------|------|------|------|------|------|------|------|
| % wt. | 89.96 | 4.32 | 1.52 | 1.88 | 0.58 | 0.47 | 0.40 | 0.30 | 0.30 | 0.21 | 0.06 |

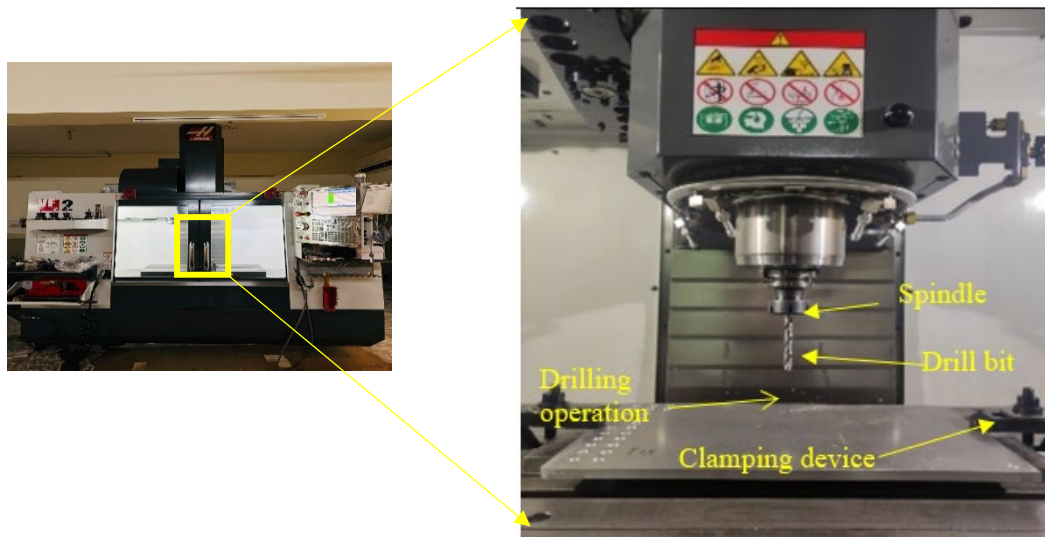


Figure 3: W/P set up on hass vf2

Drilling tests were carried out on a HAAS VF-2 CNC milling machine (40-taper spindle, 3-axis, 8100 rpm, 20-tool capacity) in dry conditions, and to avoid the use of coolants to minimize environmental/health hazards and operation costs, aiming to support sustainable practices. It was machined with an uncoated High Speed Steel (HSS) tool which was selected due to its hardness, low prices and applicability in aluminum alloys machining. HSS tools are sufficient under moderate, but not heavy, cutting conditions and allow targeted investigation of tool wear, hole quality, and tool life during dry machining (Figure 4 and 5).

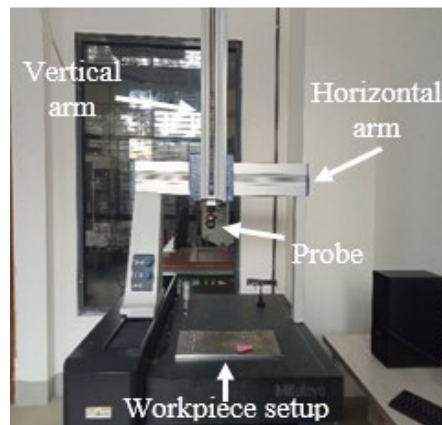


Figure 4: Measuring hole qualities (cylindricity error, circularity error) by CMM machine
Hole quality measurement was taken by CMM machine from BITAC, Dhaka Table 3 and 4).

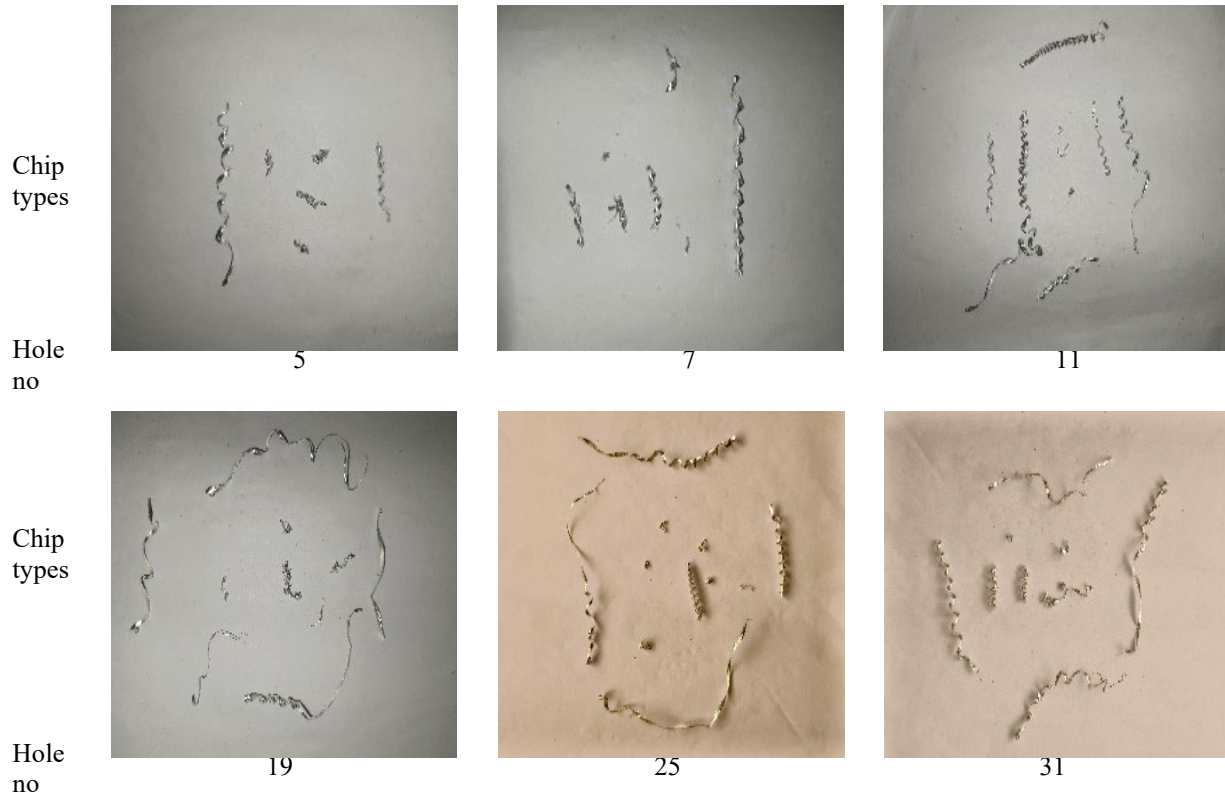
Table 3. Experimental Condition

| Category | Parameter | Value |
|-----------------------------|---------------------|-------------------|
| Work Material | Material Type | Al-5083 |
| | Workpiece Dimension | 200 × 135 × 10 mm |
| Tool | Drill Bit Type | HSS (Uncoated) |
| | Tool Diameter | 8 mm |
| | Point Angle | 118° |
| Cutting Condition | Cutting Environment | Dry |
| Machining Parameters | Spindle Speed | 3000 RPM |
| | Feed Rate | 200 mm/min |
| | Depth of Cut | 10 mm |

Table 4. Result of 52 holes Data by using HSS cutting tool on aluminum 5083 alloy

| Hole No. | M/t | Ce | Cy | Co | CT | CTR | Chip Type Description |
|----------|------|---------|--------|--------|------|----------|---|
| 1 | 3.8 | 0.011 | 0.032 | 0.01 | 0.18 | 0.157234 | curled ribbon, conical spiral, fan, segment |
| 2 | 7.6 | 0.0099 | 0.026 | 0.0085 | 0.16 | 0.176888 | loose helical, conical spiral |
| 3 | 11.4 | 0.009 | 0.02 | 0.007 | 0.21 | 0.134772 | curled ribbon, helical, conical spiral, thin ribbon |
| 4 | 15.2 | 0.0065 | 0.0195 | 0.0125 | 0.16 | 0.176888 | ribbon, loose helical, conical spiral, folded |
| 5 | 19.0 | 0.004 | 0.019 | 0.018 | 0.16 | 0.176888 | helical, conical spiral, folded |
| 6 | 22.8 | 0.003 | 0.0185 | 0.0119 | 0.18 | 0.157234 | long helical, conical spiral, fan, segment |
| 7 | 26.6 | 0.002 | 0.018 | 0.006 | 0.22 | 0.128646 | conical spiral, fan, curled ribbon |
| 8 | 30.4 | 0.0045 | 0.0219 | 0.0035 | 0.14 | 0.202158 | ribbon, segment, fan, folded spiral |
| 9 | 34.2 | 0.007 | 0.026 | 0.001 | 0.23 | 0.123053 | loose helical, curled ribbon, conical spiral, folded, segment |
| 10 | 38.0 | 0.015 | 0.0175 | 0.005 | 0.15 | 0.188681 | curled ribbon, conical spiral, segment, fan, folded |
| 11 | 41.8 | 0.023 | 0.009 | 0.009 | 0.16 | 0.176888 | conical spiral, loose helical, fan, folded, transition chip |
| 12 | 45.6 | 0.01285 | 0.0135 | 0.0055 | 0.17 | 0.166483 | curled ribbon (long), thin ribbon, segment, loose helical |
| 13 | 49.4 | 0.0027 | 0.018 | 0.002 | 0.07 | 0.404316 | thin ribbon, helical, conical spiral, fragmented chips |
| 14 | 53.2 | 0.00935 | 0.035 | 0.0015 | 0.14 | 0.202158 | long curled ribbon, conical spiral, segment, loose helical |
| 15 | 57.0 | 0.016 | 0.052 | 0.001 | 0.18 | 0.157234 | long curled ribbon, folded ribbon, segment, helical |
| 16 | 60.8 | 0.0085 | 0.041 | 0.001 | 0.14 | 0.202158 | curled ribbon, folded spiral, helical, conical spiral |
| 17 | 64.6 | 0.001 | 0.03 | 0.001 | 0.13 | 0.217709 | helical, segment, conical spiral, thin ribbon |
| 18 | 68.4 | 0.0035 | 0.0225 | 0.001 | 0.21 | 0.134772 | ribbon, conical spiral, helical, curled ribbon |
| 19 | 72.2 | 0.006 | 0.015 | 0.001 | 0.20 | 0.141511 | curled ribbon, conical spiral, transition chips, folded |
| 20 | 76.0 | 0.0105 | 0.02 | 0.001 | 0.12 | 0.235851 | thin curled ribbon, conical spiral, helical, segment |
| 21 | 79.8 | 0.015 | 0.025 | 0.001 | 0.19 | 0.148959 | curled ribbon (thin), helical, conical spiral |
| 22 | 83.6 | 0.019 | 0.0305 | 0.0165 | 0.17 | 0.166483 | curled ribbon, loose helical, conical spiral |
| 23 | 87.4 | 0.025 | 0.036 | 0.032 | 0.12 | 0.235851 | curled ribbon, transition chips, conical spiral, fan |
| 24 | 91.2 | 0.019 | 0.0245 | 0.0225 | 0.13 | 0.217709 | ribbon, folded ribbon, helical, conical spiral |
| 25 | 95.0 | 0.013 | 0.013 | 0.013 | 0.19 | 0.148959 | long ribbon, transition chips, conical spiral, segment |
| 26 | 98.8 | 0.0119 | 0.02 | 0.0065 | 0.11 | 0.257292 | long ribbon, transition chips, folded |

| | | | | | | | |
|----|-------|--------|--------|--------|------|----------|---|
| 27 | 102.6 | 0.011 | 0.027 | 0.0 | 0.14 | 0.202158 | curled ribbon, conical spiral, transition chips |
| 28 | 106.4 | 0.0069 | 0.0199 | 0.0035 | 0.07 | 0.404316 | transition chips, conical spiral, segment |
| 29 | 110.2 | 0.003 | 0.013 | 0.007 | 0.18 | 0.157234 | curled ribbon, conical spiral, transition chips |
| 30 | 114.0 | 0.005 | 0.0165 | 0.007 | 0.17 | 0.166483 | transition chips, fan, segment |
| 31 | 117.8 | 0.007 | 0.02 | 0.007 | 0.12 | 0.235851 | ribbon, transition chips, helical, segment |
| 32 | 121.6 | 0.0125 | 0.0155 | 0.005 | 0.21 | 0.134772 | ribbon, helical, conical spiral, segment |
| 33 | 125.4 | 0.018 | 0.011 | 0.003 | 0.17 | 0.166483 | folded ribbon, conical spiral, helical, segment |
| 34 | 129.2 | 0.0155 | 0.0125 | 0.0035 | 0.10 | 0.283021 | folded ribbon, folded spiral, transition chips |
| 35 | 133.0 | 0.013 | 0.014 | 0.004 | 0.17 | 0.166483 | ribbon, transition chips, conical spiral |
| 36 | 136.8 | 0.0095 | 0.03 | 0.008 | 0.16 | 0.176888 | long curled ribbon, conical spiral, fan |
| 37 | 140.6 | 0.006 | 0.046 | 0.012 | 0.19 | 0.148959 | long ribbon, conical spiral, fan, helical |
| 38 | 144.4 | 0.0145 | 0.0405 | 0.0225 | 0.11 | 0.257292 | curled ribbon, conical spiral, transition chips |
| 39 | 148.2 | 0.023 | 0.035 | 0.033 | 0.12 | 0.235851 | long curled ribbon, folded ribbon, conical spiral |
| 40 | 152.0 | 0.013 | 0.037 | 0.026 | 0.18 | 0.157234 | curled/folded ribbon, conical spiral |
| 41 | 155.8 | 0.003 | 0.039 | 0.019 | 0.08 | 0.353777 | conical spiral, helical, transition chips, ribbon |
| 42 | 159.6 | 0.0035 | 0.033 | 0.0135 | 0.06 | 0.471702 | long ribbon, conical spiral, helical |
| 43 | 163.4 | 0.004 | 0.027 | 0.008 | 0.17 | 0.166483 | curled ribbon, conical spiral, folded spiral |
| 44 | 167.2 | 0.0055 | 0.0275 | 0.0075 | 0.17 | 0.166483 | ribbon, transition chips, helical, conical spiral |
| 45 | 171.0 | 0.007 | 0.028 | 0.007 | 0.14 | 0.202158 | ribbon, helical, conical spiral |
| 46 | 174.8 | 0.011 | 0.0305 | 0.0155 | 0.12 | 0.235851 | long ribbon, helical, conical spiral |
| 47 | 178.6 | 0.015 | 0.033 | 0.024 | 0.20 | 0.141511 | conical spiral, helical, transition chips |
| 48 | 182.4 | 0.0129 | 0.0219 | 0.0185 | 0.13 | 0.217709 | curled ribbon, conical spiral |
| 49 | 186.2 | 0.011 | 0.011 | 0.013 | 0.13 | 0.217709 | thin ribbon, folded ribbon, conical spiral |
| 50 | 190.0 | 0.013 | 0.0165 | 0.0215 | 0.16 | 0.176888 | long ribbon, conical spiral, transition chips |
| 51 | 193.8 | 0.015 | 0.022 | 0.03 | 0.13 | 0.217709 | curled ribbon, conical spiral, helical |
| 52 | 197.6 | 0.0169 | 0.0275 | 0.0385 | 0.13 | 0.217709 | ribbon, conical spiral, fan |



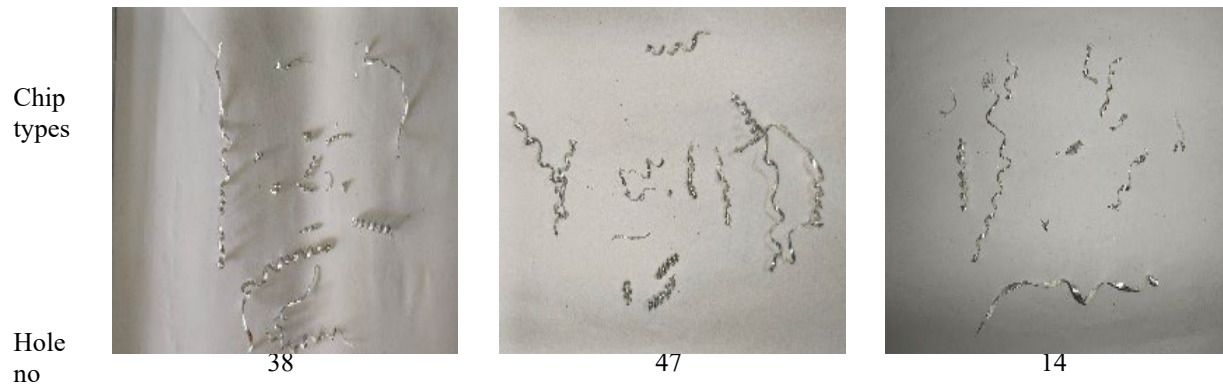


Figure 5: Chip collection of holes

4. Results And Discussion

4.1 Evidence of Progressive Tool Wear

The rate of cutting tool deterioration is the main reason behind the changes observed in chip behavior and hole quality. To better understand this process, the High Speed Steel (HSS) drill bit was observed at different stages of drilling. The photos in Figure 6 show that a large Built-Up Edge (BUE) formed at the chisel edge, which is common when cutting adhesive and ductile materials like Aluminum 5083 (Figure 6).

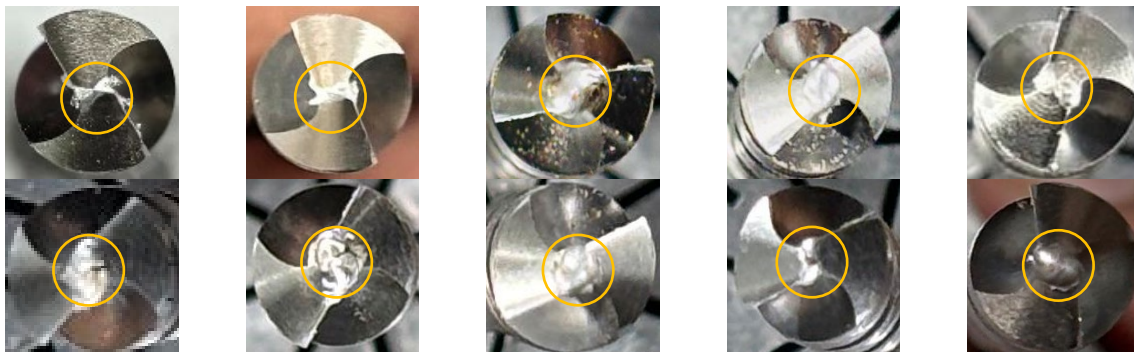


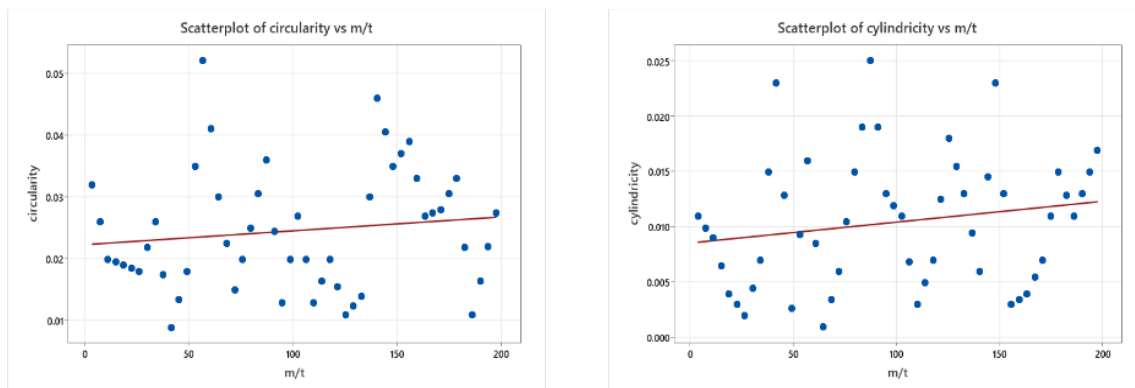
Figure 6: Progressive Formation of Built-Up Edge on the Drill Bit Tip for every 19s

This BUE causes several problems. Since it mainly forms at the chisel edge, it makes that region thicker and uneven. As a result, the drill does not sit properly on the metal surface during initial positioning. The center point loses its clean shape, so the tool struggles to stay exactly where it is placed, increasing the chance of the drill wandering at the start of the hole. The thicker chisel edge disturbs the effective cutting geometry and alters the effective rake angle, reducing shearing efficiency, increasing cutting force, and lowering hole quality. The BUE is unstable, repeatedly forming and breaking off, sometimes sticking to the chip or surface. This cycle causes the chip to shift from idealized to transition and discontinuous types. Overall, the tool degradation due to BUE directly leads to the observed changes in chip morphology and hole quality, making the process cumulative.

4.2 Analysis of Hole Quality Degradation

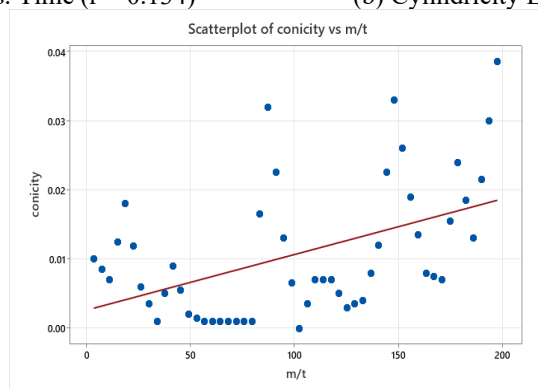
4.2.1 Correlation between Geometric Errors and Machining Time

To define the point by point correlation and measure the statistical correlation between machining time and hole quality degradation, the plot analysis was performed in detail. Circularity, Cylindricity and Conicity errors are provided in the figures below in Figure 7



(a) Circularity Error vs. Time ($r = 0.134$)

(b) Cylindricity Error vs. Time ($r = 0.185$)



(c) Conicity Error vs. Time ($r = 0.484$)

Figure 7: Correlation between Geometric Errors and Machining Time

The scatter plots show that all three geometric errors exhibit positive correlations with machining time, though with varying strengths. Figure 7(a) shows a weak positive correlation between circularity error and machining time ($r = 0.134$), while Figure 7(b) shows a similarly weak correlation for cylindricity error ($r = 0.185$). The strongest relationship appears in Figure 7(c), where conicity error shows a moderate positive correlation ($r = 0.484$), indicating that conicity tends to increase more consistently as tool wear progresses.

These differences in correlation strength can be explained by the dominant wear mechanism: the highly unstable and cyclical formation of Built-Up Edge (BUE). The instability of BUE causes fluctuating cutting forces, introducing significant noise into circularity and cylindricity measurements and masking their true positive trend. In contrast, conicity is less affected by short-term BUE fluctuations and more sensitive to the long-term cumulative wear of the cutting edges. As the drill edges gradually deteriorate, the tool can no longer maintain a uniform hole diameter, leading to a more consistent increase in conicity.

4.2.3 Inter-relationship Between Hole Quality Metrics

To better understand how hole quality degrades, pairwise relationships among the three geometric error measures were analyzed using the scatter plots in Figure 8.

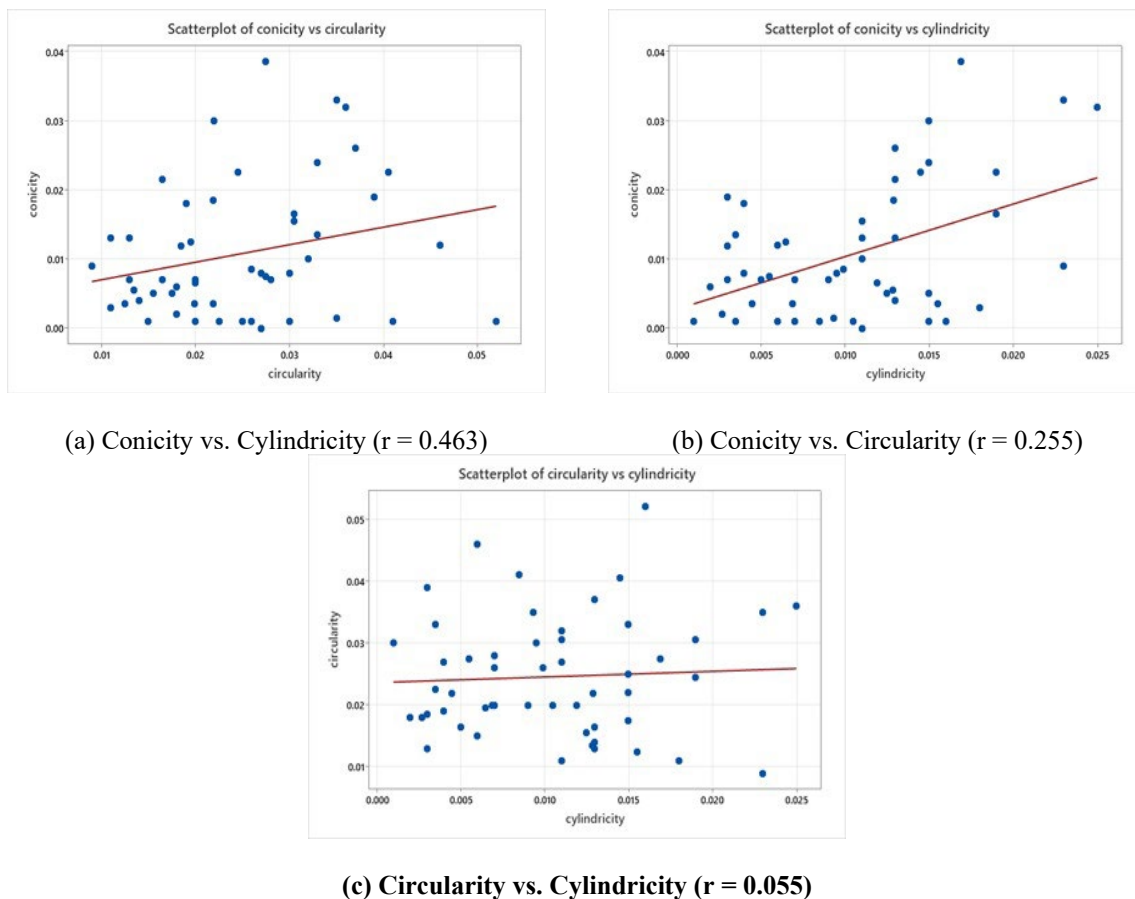


Figure 8: Inter-correlation between Geometric Error Metrics

The strongest correlation is found between cylindricity and conicity errors ($r = 0.463$), as shown in Figure 8(a). This is reasonable because both are influenced by the drill's axial stability and orientation, which gradually deteriorate due to wear at the chisel edge and cutting edges. Figure 8(b) shows a weak positive correlation between circularity and conicity errors ($r = 0.255$), indicating only a limited relationship. In contrast, circularity and cylindricity errors display almost no correlation ($r = 0.055$) in Figure 8(c). This suggests that the two metrics are governed by different physical mechanisms. Circularity is mainly affected by short-term dynamic factors—such as vibration and unstable BUE behavior at the outer cutting edges—while cylindricity reflects longer-term geometric stability and cumulative wear as the tool advances through the material. Overall, the results indicate that tool wear does not impair all aspects of hole quality uniformly; rather, each metric responds differently depending on the dominant underlying mechanism.

4.3 Analysis of Chip Behavior Evolution

Apart from hole quality, chip formation also offers important insights into the drilling process and the condition of the tool. In this section, the evolution of chip behavior is assessed through the Chip Thickness Ratio (CTR) and chip morphology.

4.3.1 Chip Thickness Ratio (CTR) vs. Machining Time

CTR represents the rate at which material is sheared during cutting. Figure 9 illustrates the relationship between CTR and cumulative machining time. The Pearson correlation coefficient is $r = 0.238$, indicating a weak positive correlation. The slightly upward trendline suggests a mild tendency for CTR to increase as tool wear progresses.

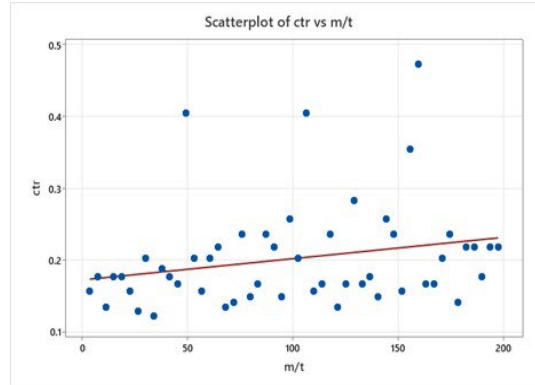


Figure 9: Correlation between CTR and Machining Time

However, the low correlation strength is noteworthy. Although BUE growth and tool wear produced clear geometric deviations in hole quality (as shown in Section 4.2), they did not yield a consistent or predictable change in the chip compression mechanism. One possible reason is that BUE accumulation can alter the effective rake angle in a complex manner, producing offsetting effects on chip thickness. This leads to high variability in CTR and masks any strong linear trend.

4.3.2 Evolution of Chip Morphology Across Machining Stages

To have more direct and qualitative estimation of tool wear, the development of chip shape was examined. The number of key chip characteristics versus the different stages of machining (0-16, 17-32, 33-48 holes) were plotted in one combined graph. This comparative analysis is given in the clustered bar chart given in Figure 10.

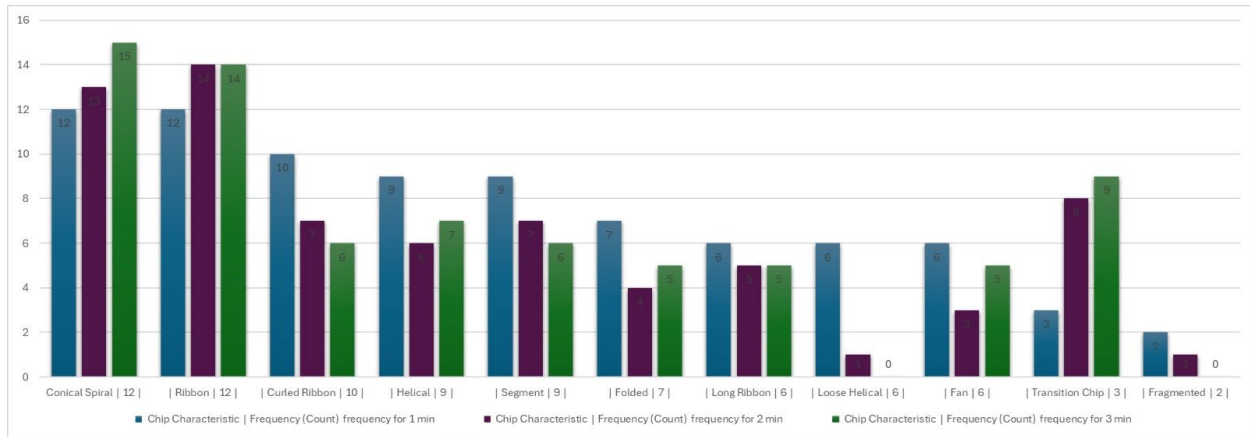


Figure 10: Comparative Frequency of Chip Characteristics

The graph indicates some of the poignant tendencies leading to the deterioration of the cutting process:

1. The most noticeable is the descent towards greater instability (Transition Chips), which goes through a low point of 3 during the first stage but peaks during the last stage of 9.
2. Perseverance of Ideal Forms: The appearance rate of ideal continuous chips such as Conical Spiral and Ribbon were very high implying that the tool did not fail farcically.
3. Trends in the discontinuous chips: Curled Ribbon discontinuous chip frequency declined over time (10 to 6), but relative to the other chips/segments it remained high.

The clustered bar chart is relevant in capturing the entire story of chip evolution and it can be used as a powerful proxy tool wear. The seemingly explosive growth in "Transition Chips" indicates a corresponding increase in the instability of the cutting process that is brought about by the periodic building up and fracturing of the BUE. With increasingly severe BUE, the property of the chip forming tool fades to stabilize its shearing and create such random-like chip

shapes. The alternation of ideal chips and discontinuous chips (such as segments) also proves that the process was not a stable one but rather oscillated between efficient cutting and inefficient ploughing process because of the worn-out state of the tool. Hence cartesian tool running (CTR) gives very poor and squishy qualitative indication compared to chip morphology about progressive tool wear.

4.4 Correlation Between Process Outputs: Chip Behavior and Hole Quality

This section examines the last connection, i.e. whether the characteristics of the chips are correlated among each other and the final hole quality.

4.4.1 Correlation between CTR and Hole Quality

To evaluate whether efficiency of chip formation (CTR) directly affected hole quality, an analysis was carried out. No statistically significant relations between CTR and any of the parameters describing the quality of holes were identified. Pearson correlation coefficients were negligible in all cases, at -0.112, 0.109 and 0.106 respectively with Cylindricity, Circularity and Conicity. This result supports the one made in Section 4.3.1. Because CTR as a measure was not strongly correlated with tool wear (machining time), then there would be no expectation that CTR would be strongly correlated to the final hole quality, which is largely a function of that wear. The hole degradation is geometric instability due to the BUE, and is not connected with the change in the chip compression ratio.

4.4.2 The Definitive Link: Impact of Chip Morphology on Hole Quality

To quantify the connection between chip formation and hole accuracy, the 52 holes were grouped into three chip types—Ideal Continuous, Transition, and Discontinuous—and their error distributions were compared using boxplots (Figure 11).

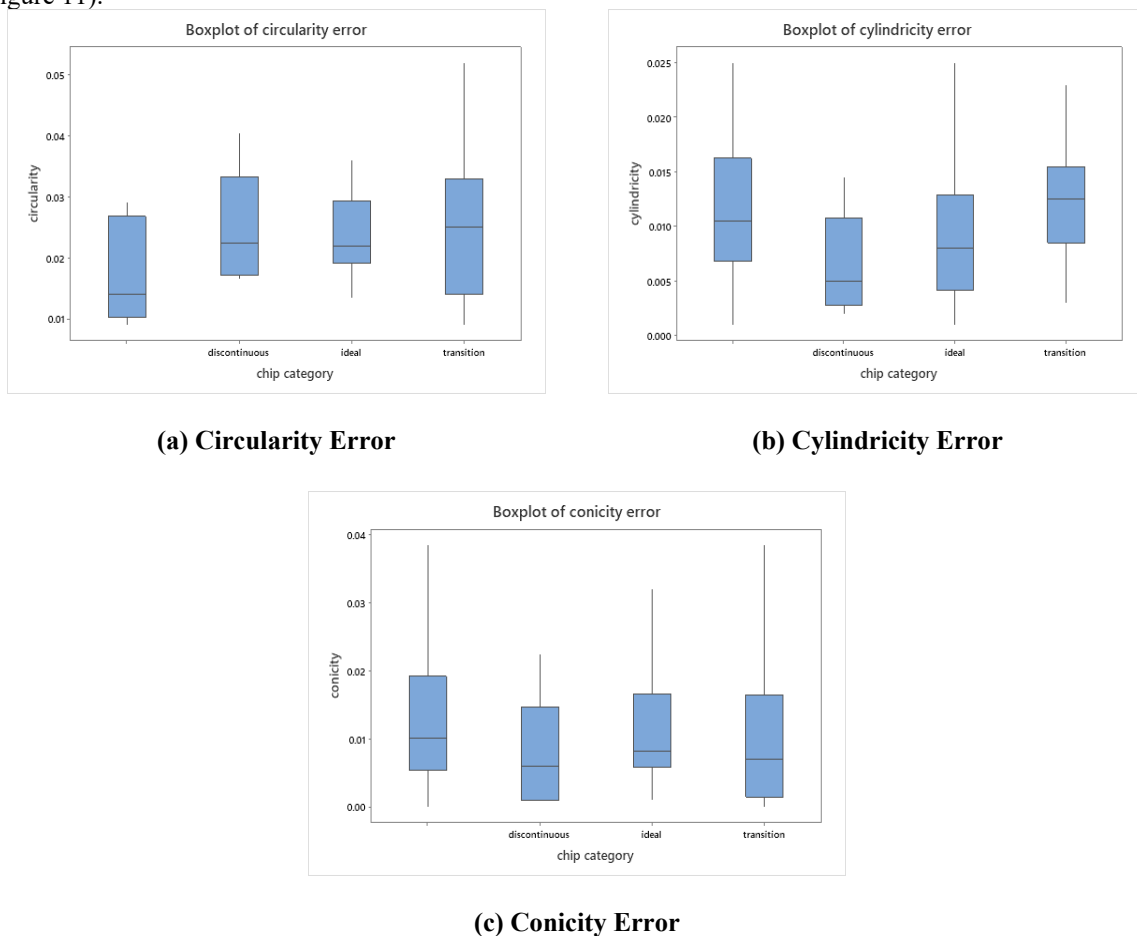


Figure 11: Distribution of Geometric Errors Grouped by Chip Category

The results show a clear relationship. For circularity in Figure 11(a), the Ideal chip group has the lowest median error and the smallest spread, indicating stable cutting. Both Transition and Discontinuous chips exhibit higher circularity errors and wider variability, showing that instability in chip formation directly affects roundness. For cylindricity and conicity in Figure 11(b–c), Discontinuous chips show somewhat lower median errors, but the Transition group consistently performs the worst, with higher medians and large spreads across all metrics. This confirms that the shift from stable to unstable chip formation is the stage where geometric accuracy deteriorates most rapidly. Overall, chip morphology acts as a practical indicator of hole quality, with Transition and Discontinuous chips serving as early warnings of tool wear and potential tolerance loss.

5. Conclusion

This study explored the evolution of drilling errors and their connection to tool wear and chip formation. Circularity and cylindricity showed only weak increases with machining time, while conicity exhibited a more consistent upward trend, reflecting its greater sensitivity to progressive tool wear. Chip morphology was found to have a direct influence on hole quality. Continuous, well-formed chips were associated with low and stable errors, whereas Transition and Discontinuous chips corresponded to higher median errors and wider variability. The Transition category, in particular, marked the stage where geometric accuracy began to deteriorate noticeably. Overall, the findings highlight that monitoring chip morphology provides a practical and real-time indicator of process stability and hole quality. Observing shifts from stable to unstable chip formation can serve as an early warning of tool wear and help maintain consistent drilling performance.

6. Limitations

Although this research possesses very useful findings, it is crucial to mention that it has some limitations. The results belong to one and the same workpiece material (Aluminum 5083) and to one type of cutting tool (HSS drill bit), along with the set of cutting parameters (speed, feed) being not varied. Hence, the results reported here have limited general applicability to other materials or machining conditions.

Acknowledgments

The authors wish to extend their profound appreciation to the conference organizing committee for offering an esteemed platform to disseminate and deliberate upon the findings of this research. The authors further acknowledge the wholehearted support of Khulna University of Engineering & Technology for facilitating the experimental and analytical components of this work and for providing the necessary financial assistance.

References

- Aamir, M., Tolouei-Rad, M., Giasin, K., and Vafadar, A., Machinability of Al2024, Al6061, and Al5083 alloys using multi-hole simultaneous drilling approach, *Journal of Materials Research and Technology*, 2020, <https://doi.org/10.1016/j.jmrt.2020.07.078>
- Aamir, M., Sharif, A., Zahir, M. Z., Giasin, K., and Tolouei-Rad, M., Experimental assessment of hole quality and tool condition in the machining of an aerospace alloy, *Machines*, Vol. 11, No. 7, 726, 2023, <https://doi.org/10.3390/machines11070726>
- Ahmad, A., Ibrahim, R., Zainoridin, H., Hong, C., and Cheng, K., An analysis of chip formation and hole circularity in drilling applications: An aircraft components perspective, *Journal of Advanced Research in Applied Mechanics*, 2024, <https://doi.org/10.37934/aram.118.1.2839>
- Akhavan Farid, A., Sharif, S., and Idris, M. H., Chip morphology study in high speed drilling of Al–Si alloy, *International Journal of Advanced Manufacturing Technology*, Vol. 57, pp. 555–564, 2011, <https://doi.org/10.1007/s00170-011-3325-3>
- Batzer, S., Haan, D., Rao, P., Olson, W., and Sutherland, J., Chip morphology and hole surface texture in the drilling of cast aluminum alloys, *Journal of Materials Processing Technology*, Vol. 79, pp. 72–78, 1998, [https://doi.org/10.1016/S0924-0136\(97\)00324-5](https://doi.org/10.1016/S0924-0136(97)00324-5)
- Davoudinejad, A., Tosello, G., and Annoni, M., Influence of the worn tool affected by built-up edge (BUE) on micro end-milling process performance: A 3D finite element modeling investigation, *International Journal of Precision Engineering and Manufacturing*, Vol. 18, No. 10, pp. 1429–1441, 2017, <https://doi.org/10.1007/s12541-017-0170-9>
- Dursun, T., and Soutis, C., Recent developments in advanced aircraft aluminium alloys, *Materials & Design*, Vol. 56, pp. 862–871, 2014, <https://doi.org/10.1016/j.matdes.2013.12.002>

- Gloria, A., Montanari, R., Richetta, M., and Varone, A., Alloys for aeronautic applications: State of the art and perspectives, *Metals*, Vol. 9, No. 6, 662, 2019, <https://doi.org/10.3390/met9060662>
- Habib, N., Sharif, A., Hussain, A., Aamir, M., Giasin, K., Pimenov, D. Y., and Ali, U., Analysis of hole quality and chips formation in the dry drilling process of Al7075-T6, *Metals*, Vol. 11, No. 6, 891, 2021, <https://doi.org/10.3390/met11060891>
- Halim, N., Dahnel, A., Ismail, A., and Zainudin, N., An experimental investigation on drilling of aluminum alloy (Al7075) using high speed steel cutting tools, 2020, <http://irep.iium.edu.my/id/eprint/80972>
- Hirsch, J., and Al-Samman, T., Superior light metals by texture engineering: Optimized aluminum and magnesium alloys, *Acta Materialia*, Vol. 61, pp. 818–843, 2013, <https://doi.org/10.1016/j.actamat.2012.10.044>
- Kao, J.-Y., Hsu, C.-Y., and Tsao, C.-C., Experimental study of inverted drilling Al-7075 alloy, *International Journal of Advanced Manufacturing Technology*, Vol. 102, pp. 3519–3529, 2019, <https://doi.org/10.1007/s00170-019-03416-8>
- Müller, C., and Blümke, R., Influence of heat treatment and cutting speed on chip segmentation of age hardenable aluminium alloy, *Materials Science and Technology*, Vol. 17, No. 6, pp. 651–654, 2001, <https://doi.org/10.1179/026708301101510519>
- Oliaei, S., and Karpat, Y., Investigating the influence of built-up edge on forces and surface roughness in micro scale orthogonal machining of titanium alloy Ti6Al4V, *Journal of Materials Processing Technology*, Vol. 235, pp. 28–40, 2016, <https://doi.org/10.1016/j.jmatprotec.2016.04.018>
- Ramme, J., Wegert, R., Guski, V., Schmauder, S., and Moehring, H.-C., Development of a multi-sensor concept for real-time temperature measurement at the cutting insert of a single-lip deep hole drilling tool, *Applied Sciences*, Vol. 12, No. 14, 7095, 2022, <https://doi.org/10.3390/app12147095>
- Sharif, A., Hussain, A., Habib, N., Alam, W., Hanif, M. I., Noon, A. A., and Khan, M. I., Experimental investigation of hole quality and chip analysis during the dry drilling process of Al6061-T6, *Journal of Materials and Manufacturing*, Vol. 2, No. 1, pp. 21–30, 2023, <https://doi.org/10.5281/zenodo.8020538>
- Shashikant Kushnoore, Noel, D., Nitin Kamitkar, and Satishkumar, M., Experimental investigations on thrust, torque and circularity error in drilling of aluminium alloy (Al6061), *American Journal of Mechanical and Industrial Engineering*, Vol. 1, No. 3, pp. 96–102, 2016, <https://doi.org/10.11648/j.ajmie.20160103.20>
- Uddin, M., Basak, A., Pramanik, A., Singh, S., Krolczyk, G. M., and Prakash, C., Evaluating hole quality in drilling of Al6061 alloys, *Metals*, Vol. 11, No. 12, 2443, 2018, <https://doi.org/10.3390/ma11122443>

Biographies

Humayra Jannat Tuba is a graduate of Industrial & Production Engineering from Khulna University of Engineering & Technology. Her interests include machining and drilling quality. She has also taken part in business case competitions and held leadership roles, blending engineering with management skills.

Dr. Mst. Nazma Sultana is an academic specializing in manufacturing, optimization, 3D printing, and simulation. She earned her B.Sc. and M.Sc. from Khulna University of Engineering & Technology and completed her Ph.D. at Bangladesh University of Engineering & Technology. She currently serves as an Associate Professor in the Department of Industrial Engineering and Management at KUET.

Nizam Uddin Ahmed is a graduate of Industrial & Production Engineering from Khulna University of Engineering & Technology, focused on drilling aluminum alloys and hole quality. He is interested in materials science and modern manufacturing research.